Monotropein alleviates H₂O₂-induced inflammation, oxidative stress and apoptosis via NF-κB/AP-1 signaling

FENG JIANG, XIAO-RONG XU, WEI-MING LI, KUN XIA, LE-FENG WANG and XIN-CHUN YANG

Heart Center and Beijing Key Laboratory of Hypertension, Beijing Chaoyang Hospital,
Capital Medical University, Beijing 100020, P.R. China

Abstract. Aging is a major risk factor in cardiovascular disease (CVD). Oxidative stress and inflammation are involved in the pathogenesis of CVD, and are closely associated with senescent vascular endothelial cells. Monotropein (Mtp) exerts various bioactive roles, including anti-inflammatory and antioxidative effects. The aim of the present study was to investigate the function of Mtp in senescent endothelial cells. An MTT assay was performed to evaluate the influence of Mtp on H_2O_2-stimulated human umbilical vein endothelial cells (HUVECs). Senescent cells were assessed by determining the expression of senescence-associated β-galactosidase, high mobility group AT-hook 1 and DNA damage marker γ-H2A.X variant histone. Malondialdehyde (MDA), superoxide dismutase (SOD), glutathione peroxidase (GSH-Px) and proinflammatory cytokine concentrations were estimated using assay kits to evaluate the levels of oxidative stress and inflammation in HUVECs. The TUNEL assay was performed to identify apoptotic cells. Furthermore, the expression levels of endothelial cell adhesion factors, NF-κB, activator protein-1 (AP-1) and apoptotic proteins were determined via western blotting. Mtp enhanced HUVEC viability following H_2O_2 stimulation. H_2O_2-mediated increases in MDA, proinflammatory cytokine and endothelial cell adhesion factor levels were decreased by Mtp treatment, whereas Mtp reversed H_2O_2-mediated downregulation of SOD and GSH-Px activity. Furthermore, Mtp inhibited cell apoptosis, NF-κB activation and AP-1 expression in H_2O_2-stimulated HUVECs; however, NF-κB activator counteracted the anti-inflammatory, antioxidative and antiapoptotic effects of Mtp. The present study indicated that Mtp ameliorated H_2O_2-induced inflammation and oxidative stress potentially by regulating NF-κB/AP-1.

Introduction

Cardiovascular disease (CVD) is a primary cause of death worldwide (1), resulting in a public health burden for society and patients. Age is considered as a major contributor to CVD, the incidence of which increases significantly with age (2,3). Vascular endothelial cells are a single layer of squamous cells covering the surface of the vascular intima, which forms the biological barrier of the vascular wall (4). Dysfunction of vascular endothelial cells is closely associated with senescence, increasing the risk of CVD in the elderly population. Senescent endothelial cells impair the function of vessels, which involves oxidative stress and a proinflammatory phenotype (5). Inflammation and oxidative stress are the primary factors of cell senescence. Inflammatory cytokines secreted by senescent cells further trigger inflammation and senescence in the surrounding tissue (6). Previous studies have demonstrated that proinflammatory cytokines are increased, and superoxide dismutase (SOD) and glutathione peroxidase (GSH-Px) activities are decreased in the process of cell senescence (6-8). Therapeutic strategies for inflammatory disorders and normalizing oxidative stress have been demonstrated to be effective in various types of CVD (9).

Monotropein (Mtp) is an iridoid glycoside isolated from the roots of *Morinda officinalis* (10). A previous study demonstrated that Mtp protected osteoblasts from H_2O_2-induced oxidative stress via regulating autophagy (11). Mtp induced the differentiation of bone marrow-derived endothelial progenitor cells and prevented cell apoptosis by decreasing the release of reactive oxygen species (ROS) (12). NF-κB is a classical transcription factor that is activated in response to extracellular stimulus, and serves a crucial role in oxidative stress and inflammatory responses (13,14). He *et al* (15) demonstrated that Mtp significantly inhibited lipopolysaccharide (LPS)-induced secretion of inflammatory cytokines by suppressing activation of the NF-κB signaling pathway. However, to the best of our knowledge, there is limited research available regarding the role of Mtp in the pathogenesis of CVD. H_2O_2-stimulated human umbilical vein endothelial cells (HUVECs) are a well-established senescent cell model (16). The aim of the present study was to simulate an oxidative environment with

Correspondence to: Dr Le-Feng Wang or Dr Xin-Chun Yang, Heart Center and Beijing Key Laboratory of Hypertension, Beijing Chaoyang Hospital, Capital Medical University, 8 Gongti South Road, Chaoyang, Beijing 100020, P.R. China
E-mail: lefw0511@163.com
E-mail: dryangxinchun@163.com

H_2O_2-stimulated vascular endothelial cells, and to determine the effects and mechanisms underlying Mtp in H_2O_2-stimulated endothelial cells.

Materials and methods

Cell culture. HUVECs (Sigma-Aldrich; Merck KGaA) were maintained in endothelial growth medium (Sigma-Aldrich; Merck KGaA) at 37˚C with 5% CO_2. HUVECs were pretreated with Mtp (0.1, 1, 10, 100 or 1,000 μM; dissolved in deionized water; purity >98%; Chengdu Herbpurify Co., Ltd.) for 24 h at 37˚C. H_2O_2 has been widely used to induce an oxidative environment in vascular endothelial cell models *in vitro* (16). To induce cell senescence, HUVECs were treated with 100 μM H_2O_2 for 12 h at 37˚C. HUVECs were incubated with 100 ng/ml phorbol 12-myristate 13-acetate (PMA; Sigma-Aldrich; Merck KGaA) for 12 h at 37˚C to activate NF-κB, as previously described (17).

MTT assay. HUVECs were seeded ($5x10^3$ cells/well) into a 96-well plate. Following treatment with H_2O_2 and Mtp, 20 μl MTT reagent (5 mg/ml; Beijing Solarbio Science & Technology Co., Ltd.) was added to each well for 4 h at 37˚C. Subsequently, 150 μl DMSO was used to dissolve the purple formazan. Absorbance was measured at a wavelength of 570 nm using a microplate reader (Bio-Rad Laboratories, Inc.).

Senescence-associated β-galactosidase (β-Gal) activity. HUVECs were collected into a centrifuge tube containing the extracting reagent of the β-Gal assay kit (Beijing Solarbio Science & Technology Co., Ltd.). HUVECs ($5x10^6$) were centrifuged at 15,000 x g for 10 min at 4˚C. The corresponding reagents in the kit were added into the tube and incubated for 30 min at 37˚C. The absorbance value was immediately determined at a wavelength of 400 nm according to manufacturer's protocol.

ELISA. Cell culture medium was centrifuged at 1,000 x g at 4˚C for 10 min. The levels of secreted IL-6, TNF-α and monocyte chemoattractant protein-1 (MCP-1) in cell culture medium were measured using human IL-6 (cat. no. EH004-48), TNF-α (cat. no. EH009-48) and MCP-1 (cat. no. EH019-48) ELISA kits (Shanghai ExCell Biology, Inc.) according to the manufacturer's protocol. Optical density values were recorded at a wavelength of 450 nm using a microplate reader (Bio-Rad Laboratories, Inc.). Each group was assessed in triplicate.

Western blotting. HUVECs were seeded ($5x10^6$) into a 100-mm petri dish. Total protein was extracted using RIPA buffer containing phosphatase inhibitors (Beijing Solarbio Science & Technology Co., Ltd.). Proteins (30 μg) were separated via 10% SDS-PAGE and transferred onto PVDF membranes (EMD Millipore). After blocking with 5% skimmed milk for 2 h at room temperature, the membranes were incubated at 4˚C overnight with primary antibodies targeted against: Phosphorylated (p)-NF-κB p65 (phosphor S276; cat. no. ab194726; 1:1,000; Abcam), NF-κB p65 (cat. no. ab16502; 1:1,000; Abcam), high mobility group AT-hook 1 (Hmga1; cat. no. ab129153; 1:20,000; Abcam), vascular cell adhesion molecule-1 (VCAM-1;

cat. no. bs-0920R; 1:500; BIOSS), intercellular cell adhesion molecule-1 (ICAM-1; cat. no. bs-4618R; 1:500; BIOSS), Bcl-2 (cat. no. bs-4563R; 1:500; BIOSS), Bax (cat. no. bs-0127R; 1:500; BIOSS), GAPDH (cat. no. bsm-33033M; 1:500; BIOSS), cleaved caspase-3 (cat. no. 9661; 1:1,000; Cell Signaling Technology, Inc.), caspase-3 (cat. no. 9662; 1:1,000; Cell Signaling Technology, Inc.), γ-H2A.X variant histone (H2AX; cat. no. 2577; 1:1,000; Cell Signaling Technology, Inc.), H2AX (cat. no. 2595; 1:1,000; Cell Signaling Technology, Inc.), p-activator protein-1 (AP-1; phospho Ser63; cat. no. ABP50261; 1:1,000; Abbkine Scientific Co., Ltd.) and AP-1 (cat. no. ABP50668; 1:1,000; Abbkine Scientific Co., Ltd.). Subsequently, the membranes were incubated with HRP-linked anti-mouse IgG (cat. no. 7076; 1:3,000; Cell Signaling Technology, Inc.) or HRP-linked anti-rabbit IgG (cat. no. 7074; 1:3,000; Cell Signaling Technology, Inc.) secondary antibodies. Protein bands were visualized using Pierce™ ECL Western Blotting Substrate (Thermo Fisher Scientific, Inc.). Protein expression levels were semi-quantified using Image Lab software (version 4.0; Bio-Rad Laboratories, Inc.).

Reverse transcription-quantitative PCR (RT-qPCR). Total RNA was extracted from cultured cells using the TRIzol® Purification kit (Invitrogen; Thermo Fisher Scientific, Inc.). Total RNA was reverse transcribed into cDNA using M-MLV Reverse Transcriptase (Promega Corporation) in the presence of oligo(dT) primers and dNTP. The following temperature protocol was used for reverse transcription: Denaturation at 70˚C for 5 min; annealing at 25˚C for 10 min; and extension at 42˚C for 50 min. Subsequently, qPCR was performed using the Power SYBR Green PCR Master mix (Thermo Fisher Scientific, Inc.) and a 7500 system (Applied Biosystems; Thermo Fisher Scientific, Inc.). The thermocycling conditions used for qPCR were as follows: 95˚C for 10 min; followed by 40 cycles of 95˚C for 15 sec and 60˚C for 60 sec. The following primers were used for qPCR: VCAM-1 forward, 5'-CAGGCT GTGAGTCCCCATT-3' and reverse, 5'-TTGACTGTGATC GGCTTCC-3'; ICAM-1 forward, 5'-ACCATCTACAGCTTT CCGGC-3'; and reverse, 5'-TTTCTGGCCACGTCCAGT TT-3'; GAPDH forward, 5'-GCACCGTCAAGGCTGAGA AC-3' and reverse, 5'-TGGTGAAGACGCCAGTGGA-3'. GAPDH was used as an internal control for quantification using the $2^{-\Delta\Delta Cq}$ method (18).

Measurement of malondialdehyde (MDA). The MDA assay kit (Beijing Solarbio Science & Technology Co., Ltd.) was used to evaluate the content of MDA. HUVECs ($4x10^6$) were collected and centrifuged at 8,000 x g for 10 min at 4˚C after adding the extracting reagent of the MDA assay kit. Subsequently, the MDA detection reagent was added and fully mixed at 100˚C for 60 min, cooled and then centrifuged at 10,000 x g for 10 min at room temperature. The supernatant (200 μl) was plated into a 96-well plate and the absorbance value was determined at wavelengths of 450, 532 and 600 nm according to the manufacturer's protocol.

Measurement of SOD. A SOD assay kit (Beijing Solarbio Science & Technology Co., Ltd.) was used to evaluate SOD activity. HUVECs ($5x10^6$) were collected and centrifuged at
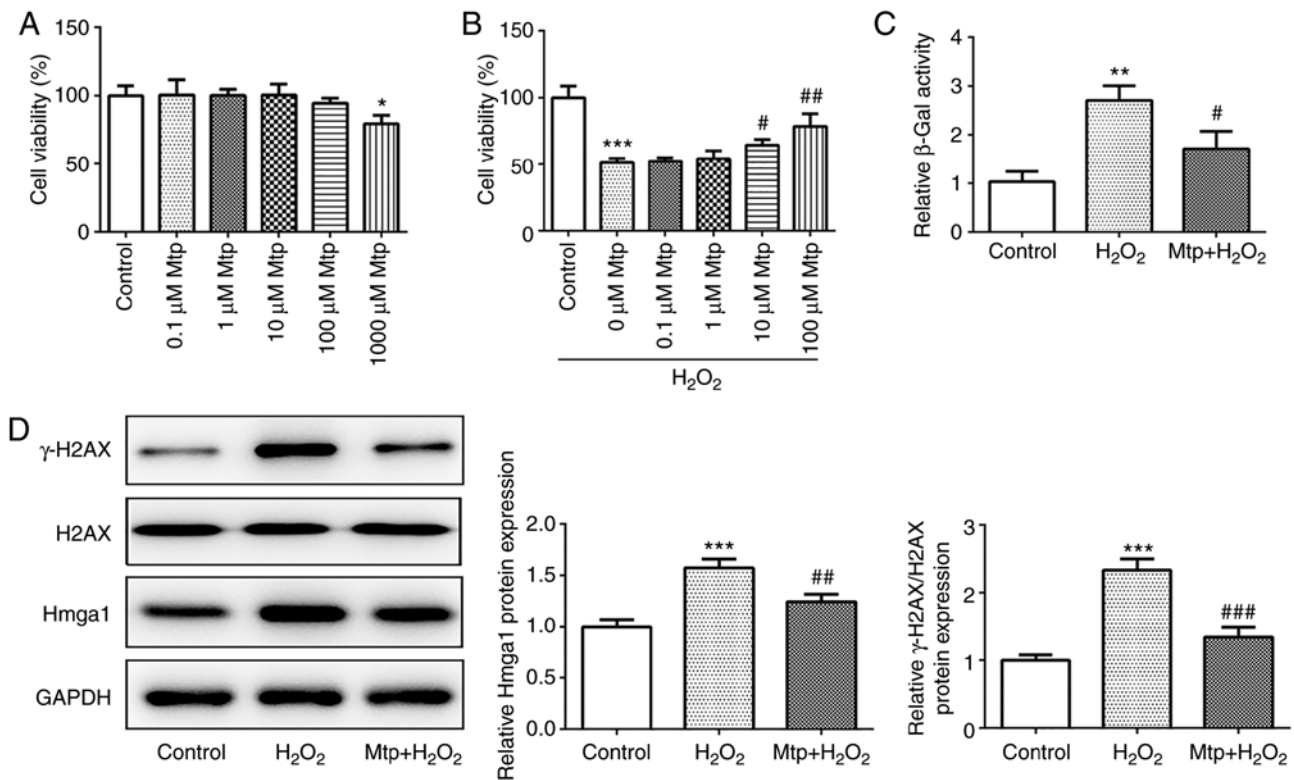
Figure 1. Mtp regulates HUVEC viability and senescence. (A) Following treatment with Mtp for 24 h, HUVEC viability was assessed by performing an MTT assay. (B) Following pretreatment with Mtp for 24 h and incubation with H_2O_2 for 12 h, HUVEC viability was assessed by performing an MTT assay. (C) Following pretreatment with 100 μM Mtp for 24 h and incubation with 100 μM H_2O_2 for 12 h, β-Gal activity was measured using a β-Gal assay kit. (D) The protein expression levels of Hmga1, γ-H2AX and H2AX were measured via western blotting. [*]P<0.05, [**]P<0.01 and [***]P<0.001 vs. control; [#]P<0.05, [##]P<0.01 and [###]P<0.001 vs. H_2O_2. Mtp, monotropein; HUVEC, human umbilical vein endothelial cell; β-Gal, β-galactosidase; Hmga1, high mobility group AT-hook 1; H2AX, H2A.X variant histone.

8,000 x g for 10 min at 4˚C after adding the extracting reagent of the SOD assay kit. Subsequently, corresponding reagents were added into the sample and fully mixed at 37˚C for 30 min. The absorbance value was measured at a wavelength of 560 nm according to the manufacturer's protocol.

Measurement of GSH-Px. The GSH-Px assay kit (Beijing Solarbio Science & Technology Co., Ltd.) was used to evaluate GSH-Px activity. HUVECs were collected and centrifuged at 8,000 x g for 10 min at 4˚C after adding the extracting reagent of the GSH-Px assay kit. Subsequently, the corresponding reagents were added into the sample and fully mixed. The absorbance value was immediately determined at a wavelength of 412 nm according to the manufacturer's protocol.

TUNEL apoptosis assay kit. Adherent cell slides were prepared to locate apoptotic cells using the TUNEL apoptosis assay kit (Nanjing KeyGen Biotech Co., Ltd.). Biotin-labeled dUTP could connect to the 3'-OH terminal of apoptotic cells via TdT Enzyme and combine specifically with streptavidin-HRP. Briefly, treated cells were fixed with fresh 4% paraformaldehyde for 15 min at room temperature, gently rinsed with PBS and incubated with 0.1% Triton X-100 for 2 min at 4˚C. The TdT enzyme was added and incubated for 60 min at 37˚C in the dark, and then with streptavidin-HRP solution for 30 min in the dark at 37˚C. Finally, diaminobenzidine solution was used to assess the color-reaction for 10 min at room temperature.

Apoptotic cells were visualized in six randomly selected fields of view using a light microscope (magnification, x200).

Statistical analysis. Data are presented as the mean ± SD. Each experiment was performed in triplicate. Statistical analyses were performed using GraphPad Prism software (version 6.0; GraphPad Software, Inc.). Comparisons between two groups were analyzed using the unpaired Student's t-test. Comparisons among multiple groups were analyzed using one-way ANOVA followed by Tukey's post hoc test. P<0.05 was considered to indicate a statistically significant difference.

Results

Mtp regulates HUVEC viability and senescence. Initially, varying concentrations of Mtp were prepared for the pretreatment of HUVECs for 24 h. The results indicated that, compared with the control group, 0.1-100.0 μM Mtp did not significantly affect HUVEC viability, but 1,000 μM Mtp significantly reduced cell viability (Fig. 1A). For subsequent experiments, 0.1-100.0 μM Mtp were used for pretreating HUVECs, which were subsequently incubated with 100 μM H_2O_2 for 12 h. The results suggested that H_2O_2 significantly inhibited cell viability in the absence of Mtp pretreatment compared with the control group. By contrast, 10 and 100 μM Mtp significantly increased cell viability in H_2O_2-stimulated HUVECs compared with the H_2O_2 group,
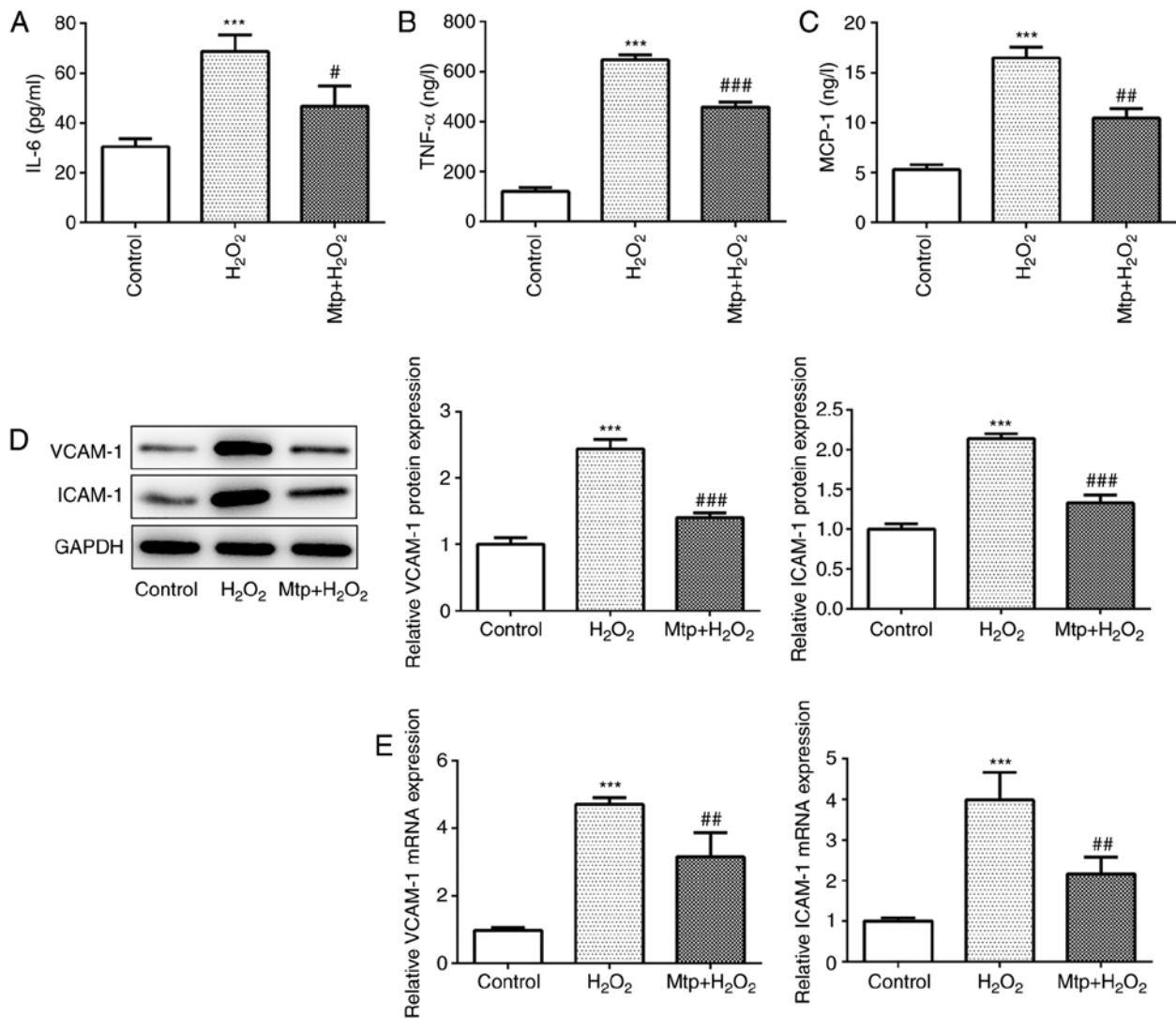
Figure 2. Mtp alleviates the inflammatory response of HUVECs. HUVECs were pretreated with 100 μM Mtp for 24 h, followed by incubation with 100 μM H$_2$O$_2$ for 12 h. The levels of secreted proinflammatory cytokines (A) IL-6, (B) TNF-α and (C) MCP-1 were determined by performing ELISAs. (D) The protein expression levels of VCAM-1 and ICAM-1 were measured via western blotting. (E) The mRNA expression levels of VCAM-1 and ICAM-1 were measured via reverse transcription-quantitative PCR. ***P<0.001 vs. control; #P<0.05, ##P<0.01 and ###P<0.001 vs. H$_2$O$_2$. Mtp, monotropein; HUVEC, human umbilical vein endothelial cell; MCP-1, monocyte chemoattractant protein-1; VCAM-1, vascular cell adhesion molecule-1; ICAM-1, intercellular cell adhesion molecule-1.

and 100 μM Mtp exhibited an improved efficacy compared with 10 μM Mtp (Fig. 1B). Subsequently, HUVECs were pretreated with 100 μM Mtp or vehicle, and then stimulated with H$_2$O$_2$ for 12 h. Compared with the control group, H$_2$O$_2$ significantly enhanced β-Gal activity, but Mtp pretreatment significantly decreased H$_2$O$_2$-induced β-Gal activity (Fig. 1C). Additionally, by measuring the expression levels of the senescence marker Hmga1 and the DNA damage marker γ-H2AX, the results also indicated that H$_2$O$_2$ increased HUVEC senescence compared with the control group, whereas Mtp pretreatment significantly inhibited H$_2$O$_2$-induced senescence (Fig. 1D). The results suggested that Mtp reversed H$_2$O$_2$-mediated downregulation of cell viability and induction of senescence.

Mtp alleviates the inflammatory response of HUVECs. To investigate the effect of Mtp on the inflammatory response in H$_2$O$_2$-stimulated HUVECs, cell culture medium was collected to estimate the release of proinflammatory cytokines, such as IL-6, TNF-α and MCP-1. The results indicated that H$_2$O$_2$ significantly upregulated the release of proinflammatory cytokines compared with the control group, and Mtp pretreatment significantly reduced H$_2$O$_2$-induced proinflammatory cytokine release, suggesting a potent anti-inflammatory effect of Mtp (Fig. 2A-C). TNF-α can cause vascular endothelial cell dysfunction, resulting in the production of a variety of cytokines, such as ICAM-1 and VCAM-1, and triggering vascular inflammation (19,20). The results indicated that ICAM-1 and VCAM-1 expression levels were significantly increased in the H$_2$O$_2$ group compared with the control group, whereas Mtp pretreatment significantly reversed H$_2$O$_2$-induced protein expression (Fig. 2D). Similarly, the mRNA levels of ICAM-1 and VCAM-1 were upregulated in the H$_2$O$_2$ group compared with the control group (Fig. 2E). Collectively, the results indicated that Mtp protected HUVECs against H$_2$O$_2$-induced inflammation.
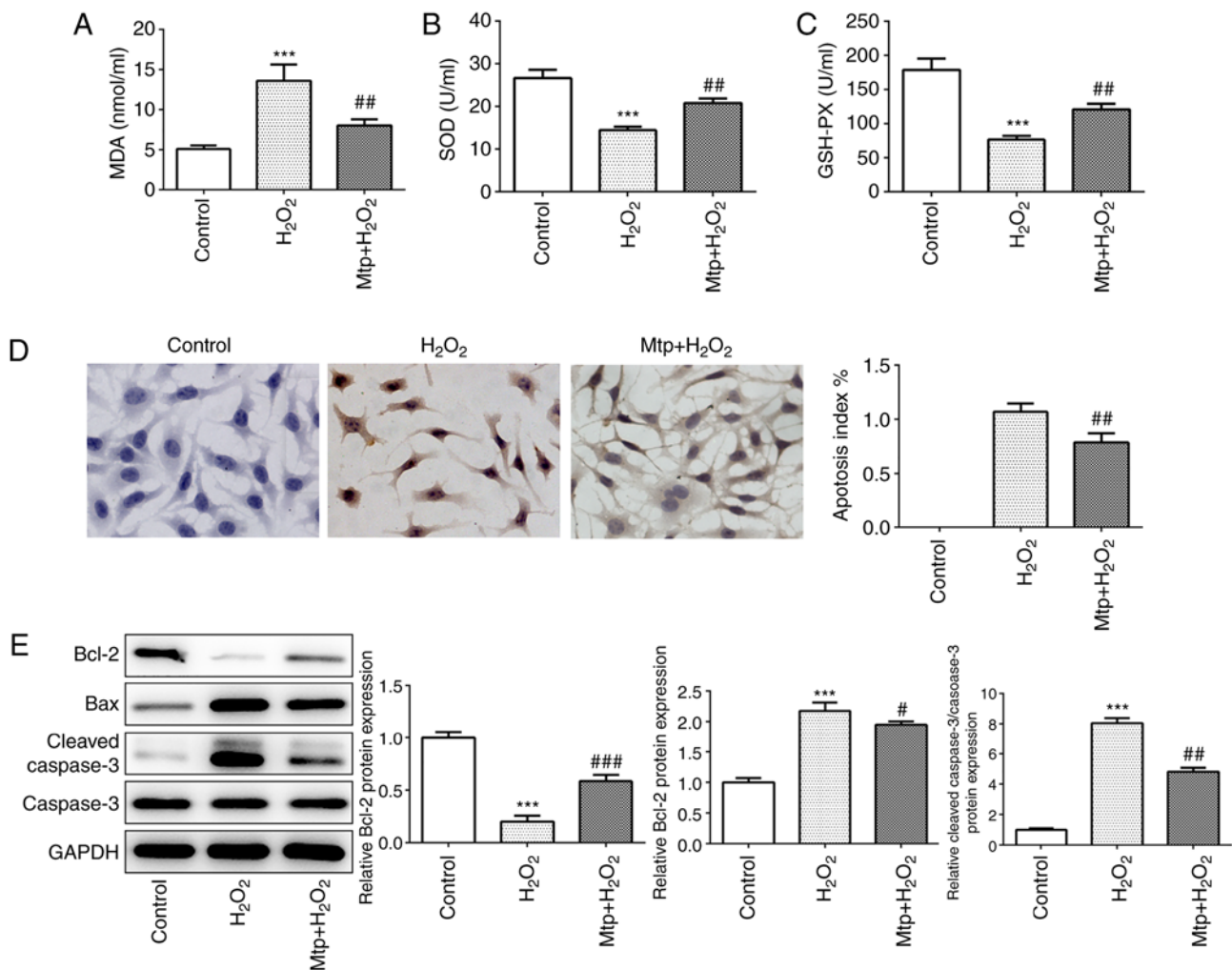
Figure 3. HUVEC oxidative stress and apoptosis are suppressed by Mtp. (A) MDA levels, and (B) SOD and (C) GSH-Px activities were determined using corresponding assay kits. (D) The TUNEL assay was performed to identify apoptotic cells (magnification, x200). Blue-stained cells represent normal HUVECs and brown-stained cells indicate apoptotic cells. (E) The protein expression levels of Bcl-2, Bax, cleaved-caspase 3 and caspase 3 were measured via western blotting. [***]$P<0.001$ vs. control; [#]$P<0.05$, [##]$P<0.01$ and [###]$P<0.001$ vs. H_2O_2. HUVEC, human umbilical vein endothelial cell; Mtp, monotropein; MDA, malondialdehyde; SOD, superoxide dismutase; GSH-Px, glutathione peroxidase.

HUVEC oxidative stress and apoptosis are suppressed by Mtp. It has previously been reported that Mtp is capable of inhibiting H_2O_2-induced ROS generation in osteoblasts (21). In the present study, MDA content was estimated to evaluate membrane lipid peroxidation. The results indicated that H_2O_2 significantly increased MDA content compared with the control group, whereas pretreatment with Mtp significantly decreased MDA levels compared with the H_2O_2 group (Fig. 3A). In addition, significantly decreased SOD and GSH-Px activities were observed in the H_2O_2 group compared with the control group, but Mtp pretreatment inhibited H_2O_2-mediated downregulation of SOD and GSH-Px activities (Fig. 3B and C), which indicated that Mtp protected HUVECs against H_2O_2-induced oxidative injury. Subsequently, whether there was an association between Mtp and cell apoptosis was investigated. The TUNEL assay indicated that apoptotic cells (brown-stained) were observed in the H_2O_2 group and Mtp pretreatment significantly decreased H_2O_2-induced cell apoptosis (Fig. 3D). Furthermore, alterations to the protein expression levels of Bcl-2, Bax and cleaved-caspase 3 indicated that Mtp pretreatment significantly relieved H_2O_2-induced cell

apoptosis (Fig. 3E). Collectively, the results indicated that Mtp ameliorated H_2O_2-induced oxidative stress and apoptosis.

Mtp anti-inflammatory effects are reversed by PMA. NF-κB is a key transcription factor associated with oxidative stress and the inflammatory response (13,14). AP-1 has been demonstrated to interact with NF-κB, and NF-κB/AP-1 signaling cascades serve an important role in inflammation (22,23). The present study suggested that the phosphorylation of NF-κB and AP-1 was significantly increased following H_2O_2 treatment compared with the control group. By contrast, pretreatment with Mtp significantly decreased the phosphorylation of NF-κB and AP-1 compared with the H_2O_2 group (Fig. 4A). PMA (100 ng/ml) was prepared and incubated with HUVECs for 12 h to activate NF-κB as previously described (17). The phosphorylation levels of NF-κB and AP-1 were significantly increased by PMA incubation compared with the control group (Fig. 4B). Furthermore, the results indicated that the anti-inflammatory effects of Mtp were significantly reversed by PMA (Fig. 4C-E), which was further indicated by significantly elevated protein expression levels of ICAM-1 and VCAM-1 in the PMA + Mtp + H_2O_2 group compared with the Mtp + H_2O_2 group
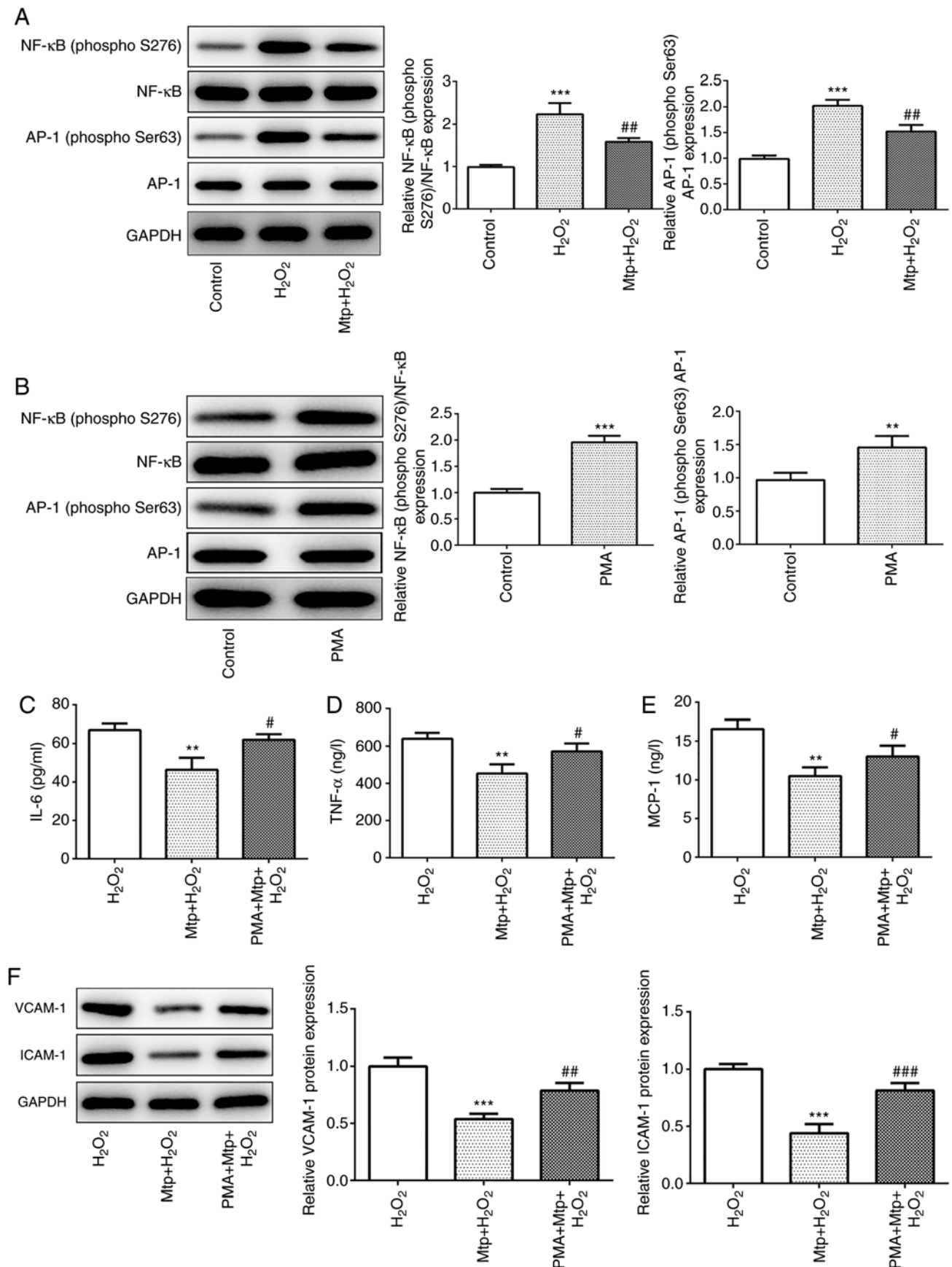
Figure 4. Mtp anti-inflammatory effects are reversed by PMA. (A) NF-κB and AP-1 protein expression levels were measured via western blotting. (B) HUVECs were treated with PMA for 12 h, and NF-κB and AP-1 protein expression levels were determined via western blotting. The levels of secreted proinflammatory cytokines (C) IL-6, (D) TNF-α and (E) MCP-1 were determined by performing ELISAs. (F) The protein expression levels of VCAM-1 and ICAM-1 were measured via western blotting. **P<0.01 and ***P<0.001 vs. control; #P<0.05, ##P<0.01 and ###P<0.001 vs. H₂O₂. Mtp, monotropein; PMA, phorbol 12-myristate 13-acetate; AP-1, activator protein-1; HUVEC, human umbilical vein endothelial cell; MCP-1, monocyte chemoattractant protein-1; VCAM-1, vascular cell adhesion molecule-1; ICAM-1, intercellular cell adhesion molecule-1.
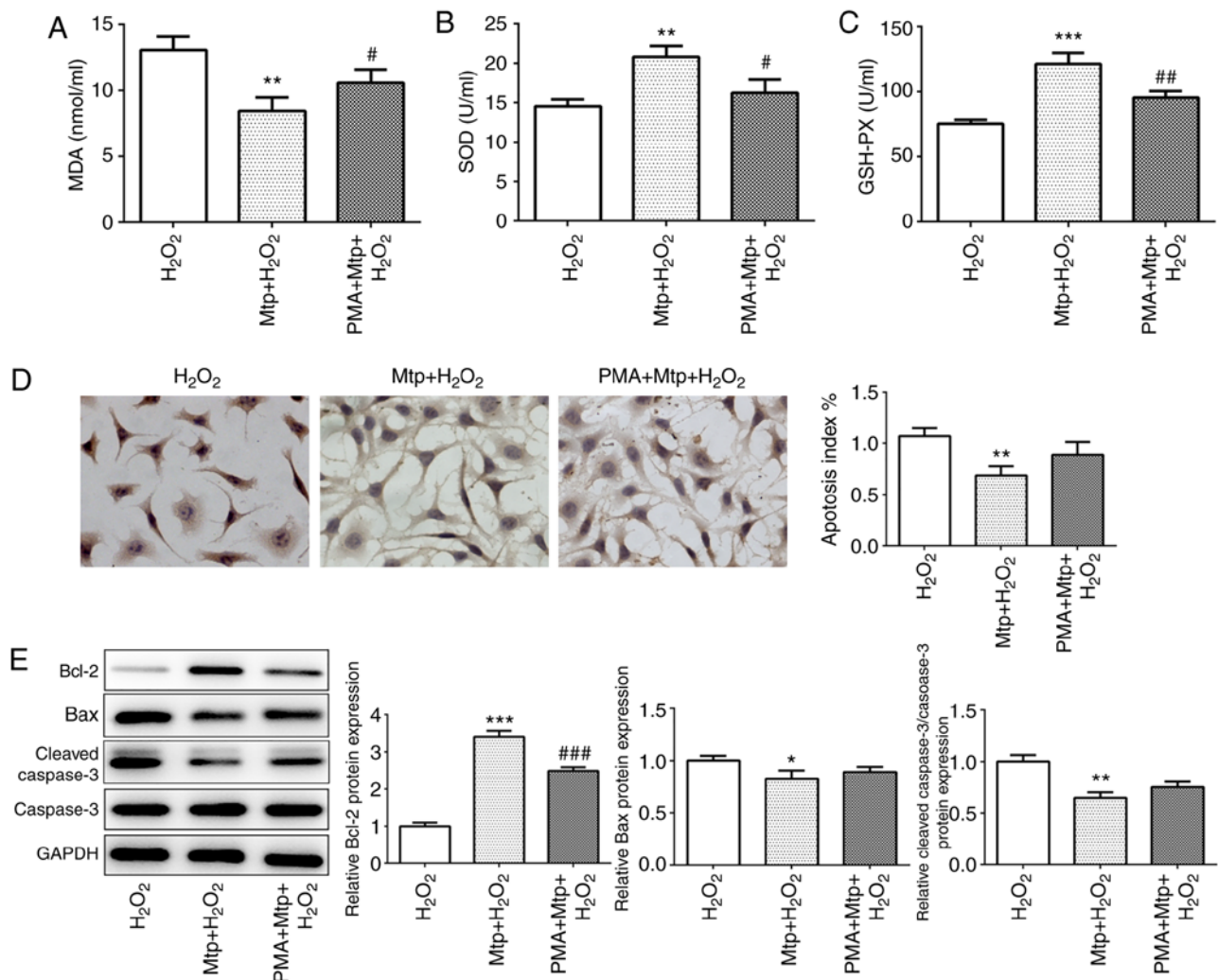
Figure 5. NF-κB/AP-1 signaling may be associated with the inhibitory effects of Mtp on HUVEC oxidative stress and apoptosis. (A) MDA levels, and (B) SOD and (C) GSH-Px activities were determined using corresponding assay kits. (D) The TUNEL assay was performed to identify apoptotic cells (magnification, x200). Blue-stained cells represent normal HUVECs and brown-stained cells indicate apoptotic cells. (E) The protein expression levels of Bcl-2, Bax, cleaved-caspase 3 and caspase 3 were measured via western blotting. $^{*}P<0.05$, $^{**}P<0.01$ and $^{***}P<0.001$ vs. H_2O_2 ; $^{#}P<0.05$, $^{##}P<0.01$ and $^{###}P<0.001$ vs. $H_2O_2 + $ Mtp. AP-1, activator protein-1; Mtp, monotropein; HUVEC, human umbilical vein endothelial cell; MDA, malondialdehyde; SOD, superoxide dismutase; GSH-Px, glutathione peroxidase.

(Fig. 4F). In summary, the results suggested that Mtp exerted an anti-inflammatory effect potentially via regulating the activation of NF-κB/AP-1 signaling cascades.

NF-κB/AP-1 signaling may be associated with the inhibitory effects of Mtp on oxidative stress and apoptosis. To further evaluate the molecular mechanism underlying HUVEC oxidative stress and apoptosis, cells were incubated with Mtp and PMA. The results suggested that Mtp pretreatment-mediated decreases in MDA content were counteracted by PMA (Fig. 5A). PMA also significantly decreased Mtp-mediated upregulation of SOD and GSH-Px in H_2O_2-stimulated HUVECs (Fig. 5B and C). In addition, Mtp pretreatment decreased H_2O_2-induced cell apoptosis, which was weakened by PMA treatment (Fig. 5D). Accordingly, Mtp-mediated downregulation of the expression levels of proapoptotic proteins Bax and cleaved-caspase 3 was reversed by PMA, whereas the protein expression levels of Bcl-2 displayed the opposite effect (Fig. 5E). The results suggested that the

inhibitory effects of Mtp on HUVEC oxidative stress and apoptosis were partially counteracted by PMA.

Discussion

Previous studies have demonstrated that Mtp exerts anti-apoptotic and anti-inflammatory effects in osteoarthritis chondrocytes (21,24,25). Nevertheless, the potential functions of Mtp in the progression of CVD are not completely understood. CVD is closely associated with senescent vascular endothelial cells, which secrete proinflammatory mediators and further exacerbate the progression of CVD (26). In the present study, HUVECs were cultured *in vitro* and stimulated with H_2O_2 to mimic a senescent cell model.

An appropriate concentration of Mtp was selected to treat HUVECs and was assessed using an MTT assay. Subsequently, by measuring the proinflammatory mediators secreted by HUVECs exposed to different stimuli, the results indicated that Mtp pretreatment ameliorated the inflammatory response

triggered by H_2O_2. In addition, the markers of oxidative stress and apoptosis were also decreased in H_2O_2-stimulated HUVECs in the presence of Mtp; however, a potential limitation of the present study may be the lack of ROS determination.

A previous study indicated that Mtp decreased the DNA binding activity of NF-κB in LPS-induced RAW 264.7 macrophages, and inhibited the phosphorylation and degradation of inhibitory κB-α, thereby inhibiting the translocation of NF-κB (27). Furthermore, Mtp inhibits the phosphorylation of NF-κB in MC3T3-E1 murine embryonic osteoblastic precursor cells (15). AP-1 is capable of interacting with NF-κB, which triggers inflammatory cytokines, including TNF-α and IL-1β, via regulating their corresponding mediator genes (28). In the present study, the phosphorylation of NF-κB was increased in H_2O_2-stimulated HUVECs compared with the control group. Pretreatment with Mtp decreased the phosphorylation of NF-κB and AP-1 in H_2O_2-stimulated HUVECs. Moreover, the results indicated that elevating the activation of NF-κB by PMA counteracted the ameliorative effects of Mtp on H_2O_2-stimulated HUVECs, suggesting that Mtp exerted its protective role by modulating the NF-κB/AP-1 signaling pathway. When cells are stimulated with PMA, the phosphorylation of p38MAPK is increased (29,30). The signaling pathway activates a variety of transcription factors, including NF-κB (p50/p65) and AP-1 (c-Fos/c-Jun), that coordinate the induction of numerous genes encoding inflammatory mediators (31), such as IL-6, TNF-α and MCP-1 (32). To date, studies on Mtp have primarily focused on osteoarthritis. He *et al* (15) demonstrated that Mtp attenuates inflammatory impairment on osteoblasts via inactivation of the NF-κB signaling pathway. Moreover, Mtp suppresses IL-1β-induced apoptosis and catabolic responses on osteoarthritis chondrocytes (24), and in Mtp-treated osteoblasts, oxidative stress was alleviated via Akt/mTOR-mediated autophagy (11). However, the role of Mtp on endothelial cells in CVD has not been previously reported.

In summary, the present study indicated that Mtp protected HUVECs against H_2O_2-induced inflammation, oxidative stress and apoptosis, potentially via mediating the NF-κB/AP-1 signaling pathway. Therefore, Mtp may serve as a candidate therapeutic for protecting HUVECs in patients with CVD via monitoring NF-κB/AP-1 signaling cascades or inhibiting NF-κB activation. The present study suggested the protective effect of Mtp on H_2O_2-induced vascular endothelial cells, indicating a potential therapeutic effect for patients with CVD via targeting endothelial functions. Nevertheless, the effects of Mtp on vascular endothelial cells were only investigated at the cellular level in the present study. Therefore, how Mtp activates NF-κB and whether Mtp affects other signaling pathways in endothelial cells requires further investigation. Moreover, animal experiments and clinical trials are required to further validate the curative effect of Mtp.

Acknowledgements

Not applicable.

Funding

Availability of data and materials

The datasets used and/or analyzed during the current study are available from the corresponding author on reasonable request.

Authors' contributions

FJ and XRX made substantial contribution to data acquisition. WML and KX contributed to data analysis. LFW and XCY designed the present study. All authors read and approved the final manuscript.

Ethics approval and consent to participate

Not applicable.

Patient consent for publication

Not applicable.

Competing interests

The authors declare that they have no competing interests.

References

1. Xue B, Head J and McMunn A: The associations between retirement and cardiovascular disease risk factors in China: A 20-year prospective study. Am J Epidemiol 185: 688-696, 2017.
2. Finegold JA, Asaria P and Francis DP: Mortality from ischaemic heart disease by country, region, and age: Statistics from world health organisation and United Nations. Int J Cardiol 168: 934-945, 2013.
3. Paneni F, Diaz Cañestro C, Libby P, Luscher TF and Camici GG: The aging cardiovascular system: Understanding it at the cellular and clinical levels. J Am Coll Cardiol 69: 1952-1967, 2017.
4. Montezano AC, Neves KB, Lopes RA and Rios F: Isolation and culture of endothelial cells from large vessels. Methods Mol Biol 1527: 345-348, 2017.
5. Pierce GL, Lesniewski LA, Lawson BR, Beske SD and Seals DR: Nuclear factor-(kappa)B activation contributes to vascular endothelial dysfunction via oxidative stress in overweight/obese middle-aged and older humans. Circulation 119: 1284-1292, 2009.
6. Serino A and Salazar G: Protective role of polyphenols against vascular inflammation, aging and cardiovascular disease. Nutrients 11: 53, 2018.
7. Salazar G, Huang J, Feresin RG, Zhao Y and Griendling KK: Zinc regulates Nox1 expression through a NF-κB and mitochondrial ROS dependent mechanism to induce senescence of vascular smooth muscle cells. Free Radic Biol Med 108: 225-235, 2017.
8. Qian Y, Zhang J, Zhou X, Yi R, Mu J, Long X, Pan Y, Zhao X and Liu W: *Lactobacillus plantarum* CQPC11 isolated from sichuan pickled cabbages antagonizes d-galactose-induced oxidation and aging in mice. Molecules 23: 3026, 2018.
9. Steven S, Frenis K, Oelze M, Kalinovic S, Kuntic M, Bayo Jimenez MT, Vujacic-Mirski K, Helmstädter J, Kröller-Schön S, Münzel T and Daiber A: Vascular inflammation and oxidative stress: Major triggers for cardiovascular disease. Oxid Med Cell Longev 2019: 7092151, 2019.
10. Zhang Z, Zhang Q, Yang H, Liu W, Zhang N, Qin L and Xin H: Monotropein isolated from the roots of *Morinda officinalis* increases osteoblastic bone formation and prevents bone loss in ovariectomized mice. Fitoterapia 110: 166-172, 2016.
11. Shi Y, Liu XY, Jiang YP, Zhang JB, Zhang QY, Wang NN and Xin HL: Monotropein attenuates oxidative stress via Akt/mTOR-mediated autophagy in osteoblast cells. Biomed Pharmacother 121: 109566, 2020.

12. Wang C, Mao C, Lou Y, Xu J, Wang Q, Zhang Z, Tang Q, Zhang X, Xu H and Feng Y: Monotropein promotes angiogenesis and inhibits oxidative stress-induced autophagy in endothelial progenitor cells to accelerate wound healing. J Cell Mol Med 22: 1583-1600, 2018.

13. Shen X, Luo L, Yang M, Lin Y, Li J and Yang L: Exendin4 inhibits lipotoxicity-induced oxidative stress in betacells by inhibiting the activation of TLR4/NF κB signaling pathway. Int J Mol Med 45: 1237-1249, 2020.

14. Wang F, Zhou H, Deng L, Wang L, Chen J and Zhou X: Serine deficiency exacerbates inflammation and oxidative stress via microbiota-gut-brain axis in D-galactose-induced aging mice. Mediators Inflamm 2020: 5821428, 2020.

15. He YQ, Yang H, Shen Y, Zhang JH, Zhang ZG, Liu LL, Song HT, Lin B, Hsu HY, Qin LP, et al: Monotropein attenuates ovariectomy and LPS-induced bone loss in mice and decreases inflammatory impairment on osteoblast through blocking activation of NF-κB pathway. Chem Biol Interact 291: 128-136, 2018.

16. Huo J, Xu Z, Hosoe K, Kubo H, Miyahara H, Dai J, Mori M, Sawashita J and Higuchi K: Coenzyme Q10 prevents senescence and dysfunction caused by oxidative stress in vascular endothelial cells. Oxid Med Cell Longev 2018: 3181759, 2018.

17. Salman I, Jung L, Adeeb S, Eun-Mi A, You L and Young L: Decursinol angelate inhibits LPS-induced macrophage polarization through modulation of the NFκB and MAPK signaling pathways. Molecules 23: 1880, 2018.

18. Livak KJ and Schmittgen TD: Analysis of relative gene expression data using real-time quantitative PCR and the 2(-Delta Delta C(T)) Method. Methods 25: 402-408, 2001.

19. Tong LT, Ju Z, Liu L, Wang L, Zhou X, Xiao T and Zhou S: Rice-derived peptide AAGALPS inhibits TNF-α-induced inflammation and oxidative stress in vascular endothelial cells. Food Sci Nutr 8: 659-667, 2020.

20. Lin CC, Pan CS, Wang CY, Liu SW, Hsiao LD and Yang CM: Tumor necrosis factor-alpha induces VCAM-1-mediated inflammation via c-Src-dependent transactivation of EGF receptors in human cardiac fibroblasts. J Biomed Sci 22: 53, 2015.

21. Zhu FB, Wang JY, Zhang YL, Hu YG, Yue ZS, Zeng LR, Zheng WJ, Hou Q, Yan SG and Quan RF. Mechanisms underlying the antiapoptotic and anti-inflammatory effects of monotropein in hydrogen peroxide-treated osteoblasts. Mol Med Rep 14: 5377-5384, 2016.

22. Jung YY, Shanmugam MK, Chinnathambi A, Alharbi SA, Shair OHM, Um JY, Sethi G and Ahn KS: Fangchinoline, a bisbenzylisoquinoline alkaloid can modulate cytokine-impelled apoptosis via the dual regulation of NF-κB and AP-1 pathways. Molecules 24: 3127, 2019.

23. Lee JH, Kim C, Lee SG, Yang WM, Um JY, Sethi G and Ahn KS: Ophiopogonin D modulates multiple oncogenic signaling pathways, leading to suppression of proliferation and chemosensitization of human lung cancer cells. Phytomedicine 40: 165-175, 2018.

24. Wang F, Wu L, Li L and Chen S: Monotropein exerts protective effects against IL-1β-induced apoptosis and catabolic responses on osteoarthritis chondrocytes. Int Immunopharmacol 23: 575-580, 2014.

25. Karna KK, Choi BR, You JH, Shin YS, Cui WS, Lee SW, Kim JH, Kim CY, Kim HK and Park JK: The ameliorative effect of monotropein, astragalin, and spiraeoside on oxidative stress, endoplasmic reticulum stress, and mitochondrial signaling pathway in varicocelized rats. BMC Complement Altern Med 19: 333, 2019.

26. Donato AJ, Morgan RG, Walker AE and Lesniewski LA: Cellular and molecular biology of aging endothelial cells. J Mol Cell Cardiol 89: 122-135, 2015.

27. Shin JS, Yun KJ, Chung KS, Seo KH, Park HJ, Cho YW, Baek NI, Jang D and Lee KT: Monotropein isolated from the roots of Morinda officinalis ameliorates proinflammatory mediators in RAW 264.7 macrophages and dextran sulfate sodium (DSS)-induced colitis via NF-κB inactivation. Food Chem Toxicol 53: 263-271, 2013.

28. Han Y, Li X, Zhang X, Gao Y, Qi R, Cai R and Qi Y: Isodeoxyelephantopin, a sesquiterpene lactone from Elephantopus scaber Linn., inhibits pro-inflammatory mediators' production through both NF-κB and AP-1 pathways in LPS-activated macrophages. Int Immunopharmacol 84: 106528, 2020.

29. Zhang T, Chen T, Chen P, Zhang B, Hong J and Chen L: MPTP-induced dopamine depletion in basolateral amygdala via decrease of D2R activation suppresses GABA$_A$ receptors expression and LTD induction leading to anxiety-like behaviors. Front Mol Neurosci 10: 247, 2017.

30. Alvarez SE, Milstien S and Spiegel S: Autocrine and paracrine roles of sphingosine-1-phosphate. Trends Endocrinol Metab 18: 300-307, 2007.

31. Gay NJ and Gangloff M: Structure and function of toll receptors and their ligands. Annu Rev Biochem 76: 141-165, 2007.

32. Sperlich J, Kerr R and Teusch N: The marine natural product pseudopterosin blocks cytokine release of triple-negative breast cancer and monocytic leukemia cells by inhibiting NF-κB signaling. Mar Drugs 15: 262, 2017.